

University of Groningen

Soft tissue aneurysmal bone cyst

Song, Wangzhao; Suurmeijer, Albert J. H.; Bollen, Stijn M.; Cleton-Jansen, Anne-Marie; Bovee, Judith V. M. G.; Kroon, Herman M.

Published in:
 Skeletal Radiology

DOI:
[10.1007/s00256-018-3135-x](https://doi.org/10.1007/s00256-018-3135-x)

IMPORTANT NOTE: You are advised to consult the publisher's version (publisher's PDF) if you wish to cite from it. Please check the document version below.

Document Version
 Publisher's PDF, also known as Version of record

Publication date:
 2019

[Link to publication in University of Groningen/UMCG research database](#)

Citation for published version (APA):

Song, W., Suurmeijer, A. J. H., Bollen, S. M., Cleton-Jansen, A-M., Bovee, J. V. M. G., & Kroon, H. M. (2019). Soft tissue aneurysmal bone cyst: six new cases with imaging details, molecular pathology, and review of the literature. *Skeletal Radiology*, *48*(7), 1059-1067. <https://doi.org/10.1007/s00256-018-3135-x>

Copyright

Other than for strictly personal use, it is not permitted to download or to forward/distribute the text or part of it without the consent of the author(s) and/or copyright holder(s), unless the work is under an open content license (like Creative Commons).

The publication may also be distributed here under the terms of Article 25fa of the Dutch Copyright Act, indicated by the "Taverne" license. More information can be found on the University of Groningen website: <https://www.rug.nl/library/open-access/self-archiving-pure/taverne-amendment>.

Take-down policy

If you believe that this document breaches copyright please contact us providing details, and we will remove access to the work immediately and investigate your claim.

Downloaded from the University of Groningen/UMCG research database (Pure): <http://www.rug.nl/research/portal>. For technical reasons the number of authors shown on this cover page is limited to 10 maximum.



Soft tissue aneurysmal bone cyst: six new cases with imaging details, molecular pathology, and review of the literature

Wangzhao Song¹ · Albert J. H. Suurmeijer¹ · Stijn M. Bollen² · Anne-Marie Cleton-Jansen³ · Judith V. M. G. Bovée³ · Herman M. Kroon²

Received: 1 October 2018 / Revised: 28 November 2018 / Accepted: 10 December 2018 / Published online: 2 January 2019
© ISS 2019

Abstract

Objective Aneurysmal bone cysts (ABC) rarely present in soft tissue locations (STABC). The 30 cases of STABC reported in the English literature were reviewed. Six new cases retrieved from the files of the Netherlands Committee on Bone Tumors were compared to the six cases described in the radiological literature.

Materials and methods Imaging studies and histopathology of six new STABC cases were reviewed. Follow-up was recorded with respect to local recurrence. FISH for *USP6* rearrangement and/or anchored multiplex PCR-based targeted NGS using Archer FusionPlex Sarcoma Panel were attempted.

Results On imaging, the six STABC cases presented as a solid or multicystic intramuscular soft tissue mass, usually with thin peripheral mineralized bone shell. On MRI, perilesional edema was visualized in nearly all cases. Fluid-fluid levels were observed in one case. All lesions had the distinct histologic features of STABC. In three cases suitable for NGS, the diagnosis of STABC was confirmed by a *COL1A1–USP6* fusion gene. In one additional case, *USP6* gene rearrangement was detected by FISH. After marginal excision, none of the six STABC recurred after a mean follow-up period of 50 months (range, 39–187 months).

Conclusions On imaging, it can be difficult to discriminate between STABC and myositis ossificans. The presence of a thin bony shell and fluid-fluid levels can be helpful in discriminating these two entities. STABC is readily diagnosed after histopathologic examination of the resection specimen. STABC belongs to the spectrum of tumors with *USP6* rearrangements, which includes ABC, myositis ossificans, and nodular fasciitis.

Keywords Soft tissue · Aneurysmal bone cyst · *USP6* · Radiography · CT · MRI · Ultrasound · Radionuclide imaging

Introduction

Aneurysmal bone cyst (ABC) is a distinct bone tumor, which is either primary or secondary to another tumor or tumor-like lesion of bone. Primary ABC usually occurs in children and adolescents. The most common sites are the metaphysis of the

long tubular bones and the posterior elements of the vertebrae, where it usually presents as a relatively well-defined osteolytic lesion, often with expansion of the bone and fluid-fluid levels on MR imaging [1]. Aneurysmal bone cyst rarely occurs as a primary soft tissue tumor (STABC). Salm and Sissons (1972) [2] were the first to describe two cases of extraskeletal giant-cell-containing lesions with histological features identical to ABC of bone. To our knowledge, only up to 30 cases of STABC were reported in the English literature to date. Thus far, only six have been reported in the radiological literature [3–8]. In this article, we describe imaging and histopathologic features of six new cases of primary STABC. Moreover, molecular studies (FISH and anchored multiplex PCR-based targeted NGS, using the Archer FusionPlex Sarcoma kit) were done in an attempt to demonstrate specific gene fusions of ABC. We compared our findings to those reported in the literature.

✉ Herman M. Kroon
h.m.j.a.kroon@lumc.nl

¹ Department of Pathology and Medical Biology, University Medical Center Groningen, University of Groningen, Groningen, The Netherlands

² Department of Radiology, C-2-S, Leiden University Medical Center, PO Box 9600, 2300RC Leiden, The Netherlands

³ Department of Pathology, Leiden University Medical Center, Leiden, The Netherlands

Materials and methods

Patient data

The six STABC cases were retrieved from the files of the Netherlands Committee on Bone Tumors. Imaging studies and histopathologic features of the cases were reviewed by experienced radiologists and pathologists, respectively. Follow-up was recorded with respect to local recurrence.

Conventional radiography was available in all six cases, MR imaging in five cases (except case 5), MR + contrast-enhanced MR were performed in three cases (cases 1, 2, 3). CT + radionuclide imaging was available in three patients (case 4: CT + SPECT; case 5: CT + conventional radionuclide imaging; case 6: CT + PET-CT), whereas ultrasonography was done in two cases (cases 1, 3).

In each case, formalin-fixed, paraffin-embedded material was available for review. The study was performed in accordance with the code of conduct for responsible use of human tissue that is used in the Netherlands (Dutch Federation of Biomedical Scientific Societies; <http://www.federa.org>).

FISH

A commercial fusion probe (Kreatech, Amsterdam, the Netherlands) that detects USP6 rearrangements was used to do fluorescence in situ hybridization (FISH). Three- μ m-thick FFPE slides were deparaffinized and ethanol dehydrated, and FISH was performed using the Histology Fish Accessory Kit (Dako, Glostrup, Denmark), as per the manufacturer's description. Slides were counterstained with 10 μ l of 4',6-diamidino-2-phenylindole (DAPI) before visualization and quantification (200 nuclei) by fluorescence microscopy. Two hundred nuclei of the spindle cells were counted for the presence of break-apart signals. When at least ten nuclei with a break apart signal are observed, this is considered as an USP6 translocation. This is a lower threshold than for other translocations, because in STABC it is difficult to distinguish lesional cells from non-lesional cells.

Targeted next-generation sequencing (NGS) based on anchored multiplex PCR (AMP)

Total nucleic acid (DNA and RNA) was isolated from 50- μ m FFPE slides using the TPS (tissue preparation system) (Siemens), as described previously [9]. A target-enriched cDNA library was prepared with the Archer® FusionPlex® Sarcoma kit as described by the manufacturer (<http://archerdx.com/fusionplex-assays/sarcoma>). In short, reverse transcription of RNA was followed by end repair, adenylation, and universal half-functional adapter ligation of double-stranded cDNA fragments. This was followed by two rounds of low-cycle PCR with universal primers and gene-specific primers, covering 26 target genes that rendered the library fully functional for clonal amplification and sequencing using the Ion Proton™ system. With the Archer-DX analysis software, the libraries were analyzed for presence of relevant fusions and in their absence sequence quality was assessed by the manufacturer's criteria.

Results

Clinicopathologic features

Four female and two male patients were included in this study (Table 1). Their age ranged from 15 to 49 years (mean age, 27 years, median age, 25.5 years). All patients presented with a painful mass without a history of previous trauma in any of them. Four lesions were located in the upper leg; the remaining two were located in the lower abdominal wall and anterior pelvic region. All tumors were excised with narrow margins. On gross examination, tumor size ranged from 2.5 to 8.0 cm (mean size, 4.5 cm). In all but one case, STABC was a multilocular cystic tumor. One case was predominantly solid and had one small cyst. Microscopically, the distinctive appearance of STABC included areas with blood-filled cysts and septa (Fig. 1a, f) or more solid areas (Fig. 1b) with bland spindle cells and osteoclastic giant cells. In case 3, the

Table 1 Distinct histologic features of our six STABC cases

Case	Age/ sex	Location, muscle	Size	Solid/cystic	Blue bone	USP6 FISH	NGS	FU/ NED
1	49/F	Biceps femoris	4.5 cm	Cystic	No	Yes	COL1A1-USP6	42 mo
2	34/F	Vastus lateralis	4.0 cm	Cystic	Yes	NP	COL1A1-USP6	57 mo
3	15/M	Vastus medialis	2.5 cm	Cystic	Yes	Failure	Failure	39 mo
4	19/F	Vastus medialis	4.0 cm	1 small cyst	Yes	NP	COL1A1-USP6	50 mo
5	16/F	Oblique transverse abdominal	8.0 cm	Cystic	No	Yes	NP	187 mo
6	32/M	Gluteus minimus	4.0 cm	Cystic	Yes	Failure	Failure	45 mo

NP not performed, FU follow-up, NED no evidence of disease, mo month

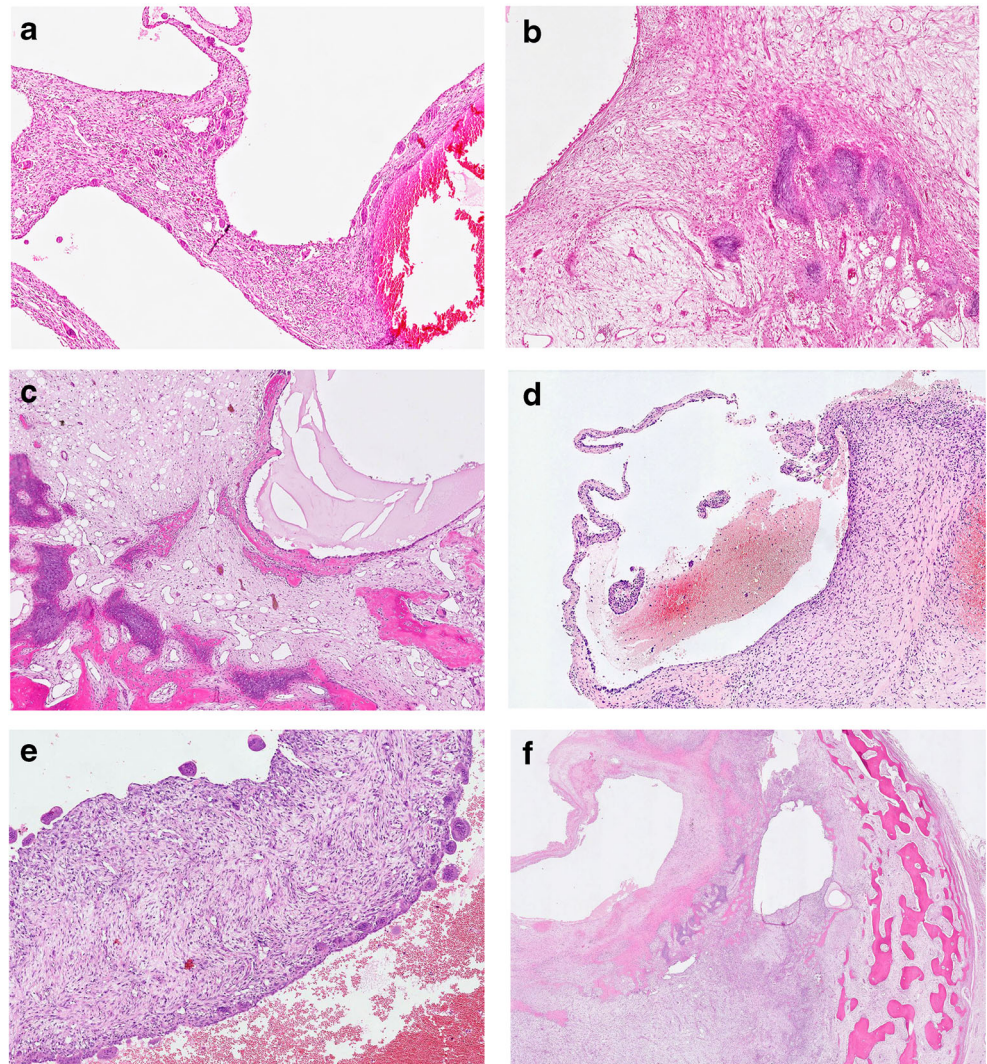
multilocular cysts were filled with proteinaceous fluid (Fig. 1c). Mitotic activity or nuclear atypia were absent. In the tumor border zone, a shell of mature lamellar bone was formed via differentiating areas of woven bone surrounded by osteoblasts (Fig. 1f). Blue osteoid bone matrix was found in four cases (Fig. 1b, c, and f). Notably, case 4 showed a distinct histological feature compared with other cases. Grossly, this tumor was located in skeletal muscle had a 1-cm-thick peripheral bone shell (Fig. 2). In the center, only glistening myxoid tissue was discerned and cystic cavities were absent. By histology, this central area was composed of loose myxoid stroma with focal cellular areas with myofibroblasts, hemosiderin, and osteoclast-like giant cells (Fig. 1d). There was an extensive formation of woven trabecular bone with peripheral maturation and formation of lamellar bone surrounded by osteoblasts, a morphology reminiscent of myositis ossificans. However, the previous needle biopsy material contained a small cystic area with distinct histological features of STABC. On clinical follow-up, none of the tumors recurred.

Imaging

Imaging findings of six STABCs are summarized in Table 2. Ultrasound examination was performed in two cases, which showed a calcified cystic lesion with acoustic shadowing (case 1 and 3, Fig. 3). Conventional radiography revealed a relatively well-demarcated soft tissue mass surrounded by a bone shell (Fig. 4a, b). None of the tumors originated from or was connected to the underlying bone.

On MRI, STABC presented as a lobulated soft tissue mass with a predominantly intermediate signal intensity on T1-weighted images (Fig. 5a, b). In one case, the signal intensity on the T1-weighted sequences was predominantly high with fluid-fluid levels consistent with blood-filled cystic spaces (Fig. 5a). On T2-weighted images with fat suppression, there was heterogeneous, predominantly high signal intensity (Fig. 5c, d). After intravenous contrast administration, there was a heterogeneous diffuse enhancement of the mass in two patients (cases 2 and 3) and septal enhancement in one (case 1,

Fig. 1 Microphotographs of the six STABC cases (a–f) corresponding to case 1–6) described (H&E stain). STABC has blood-filled cysts and septa (a, f) or more solid areas (b) with bland spindle cells and osteoclast-type giant cells. Woven bone deposited along the cyst cavity (c, d) is a typical feature and blue bone (b, c, f) is considered to be a hallmark of STABC. At the border area, the peripheral bone shell consisted of mature trabecular bone (f)



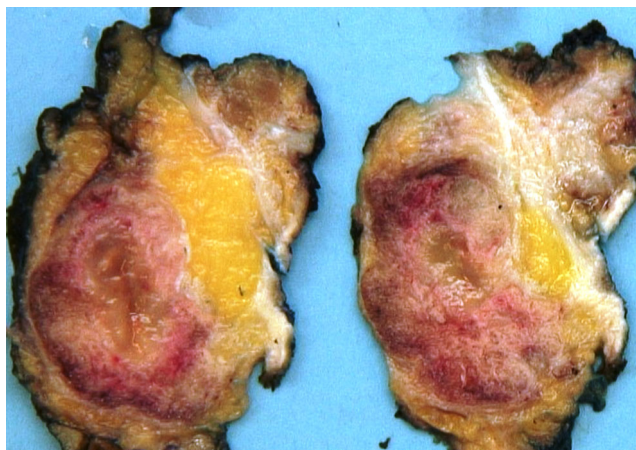


Fig. 2 Gross features of case 4, the tumor with thick peripheral bone shell, glistening myxoid tissue in the center and absent cystic cavities

Fig. 5e). Perilesional edema was observed in all five patients with MR imaging, with extensive ill-defined high signal intensity in the adjacent muscle beyond the periphery of the mass (Fig. 5c–e). Fluid–fluid levels were evident in one case. In all five patients with MR, on all sequences, a peripheral hypo-intense rim, corresponding with the peripheral mineralization, was visualized. On CT, a shell of peripheral mineralization was demonstrated in cases 4, 5, and 6 (Fig. 6). A technetium-99 m-MDP bone study in case 5 demonstrated increased uptake of the radiotracer, predominantly in the periphery, whereas a SPECT study showed intense uptake of the radiopharmakon throughout the lesion (Fig. 7). A PET-CT performed in case 6 showed a soft tissue mass surrounded by a bony shell with variable thickness from thin to intermediate, but predominantly thin. There was markedly increased uptake of the radiopharmakon at the periphery of the lesion (Fig. 8).

Molecular analysis

In two cases, *USP6* gene rearrangement was detected by *USP6* break-apart FISH assay (cases 1 and 5). In three cases (cases 1, 2, and 4) suitable for analysis, a fusion of exon1 of *COL1A1* with exon 1 of *USP6* was found with anchored multiplex PCR-based targeted NGS. Due to acid decalcification and subsequent DNA denaturation, it was not possible to perform FISH and NGS in cases 3 and 6. However, as shown in Fig. 1c and f, the histology was typical of STABC.

Discussion

Jaffe and Lichtenstein (1942) [1] were the first to describe aneurysmal bone cyst (ABC), a benign, locally aggressive, and expansile lesion that typically occurs in the long tubular bones or vertebrae of children and young adults, both male and female [1, 10, 11]. ABC of bone can occur as a primary lesion or be associated with a pre-existing bone condition such as chondroblastoma, giant cell tumor, fibrous dysplasia, and even osteosarcoma [12]. In these cases, ABC is considered to be secondary. Radiographically, the characteristics of a primary ABC of bone are an osteolytic lesion, usually eccentrically, expansile with well-defined margins, and predominantly located in the metaphysis of long tubular bones or the posterior elements of vertebrae.

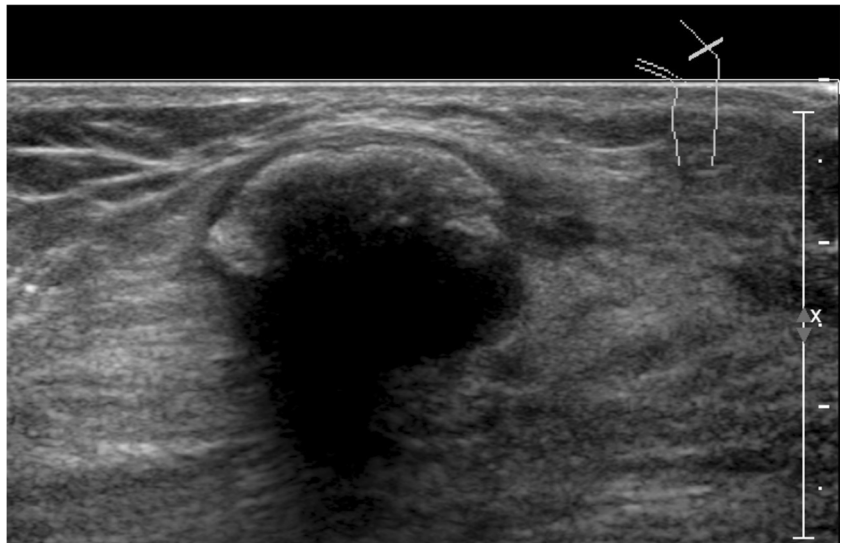
Aneurysmal bone cyst has a soft tissue counterpart. Soft tissue ABC (STABC) was first reported by Salm and Sissons in 1972 [2]. Since then, only up to 30 cases have been reported in the English literature, with only six cases published in the radiological literature [3–8]. We add six more cases and reviewed the literature with regard to clinical presentation,

Table 2 Imaging features of 12 cases of STABC, including the six cases described herein

Case	Author	Bone shell on radiograph and/or CT	Multicystic/solid (CT, MR)	Fluid–fluid levels (MR)	Septal enhancement (MR)	Perilesional edema on MR	Gross pathology
1	Amir	Yes, thick	Solid	NP	NP	NP	Multicystic
2	Samura	No	Multicystic	No	NP	Yes	Multicystic
3	Wang	Yes, thin	Multicystic	Yes	Yes	Yes	Multicystic
4	Ajilogba	No	Solid	No	No	Yes	Multicystic
5	Jacquot	Yes, thin	Multicystic	Yes	NP	No	Multicystic
6	Baker	Yes, thin	Multicystic	Yes	Yes	Yes	Multicystic
7	Case 1	Yes, thin	Multicystic	Yes	Yes	Yes	Multicystic
8	Case 2	Yes, thin	Solid	No	No	Yes	Multicystic
9	Case 3	Yes, thin	Solid	No	No	Yes	Multicystic
10	Case 4	Yes, thick	Solid	No	NP	Yes	1 small cyst
11	Case 5	Yes, thin	Probably cystic	NP	NP	NP	Multicystic
12	Case 6	Yes, thin	Multicystic	No	NP	Yes	Multicystic

NP not performed

Fig. 3 Ultrasound image with highly reflective shell and acoustic shadowing caused by the peripheral calcification (case 3)



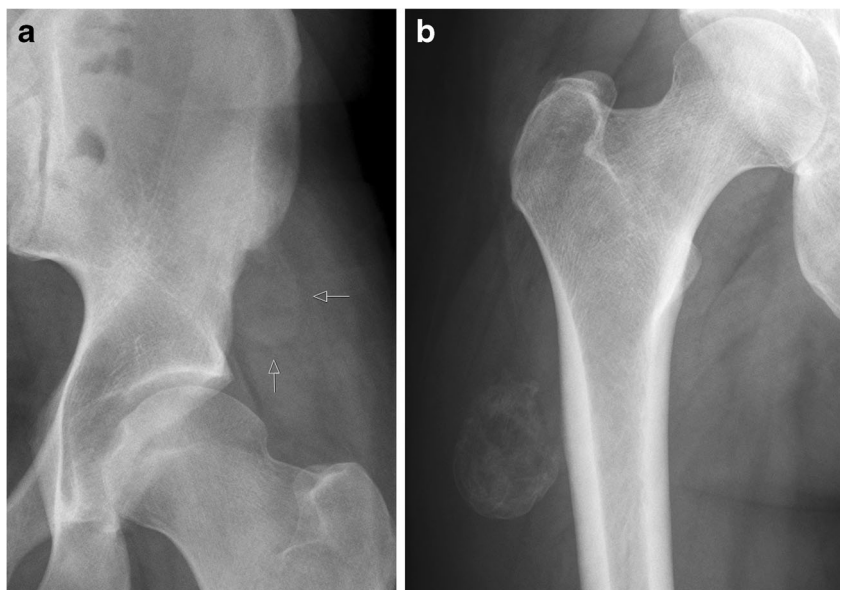
tumor localization, radiological features, as far as these could be derived from the text and/or available illustrations, and follow-up.

Clinical features of STABC

Reviewing the literature [1–8, 13–29], patients with STABC presented with a painless or tender, slow-growing mass, with a mean size of 5.5 cm (range, 2–12 cm). The vast majority of patients indicated no previous trauma (30/36; 83.3%). Remarkably, in two patients, STABC occurred in an area of previous surgery [2, 16]. There was a female predominance; 22/36 (61.1%). Mean age and median age at presentation were 28.7 and 27 years, respectively, which is higher than that of

patients with ABC of bone (75% of the patients with primary ABC of bone are younger than 20). The lesions were mainly located in the upper leg, groin, or buttock region (15/36, 41.7%), followed by upper arm and shoulder region (9/36, 25.0%). Other locations reported are the retroclavicular region, breast, common carotid artery, pelvic cavity, cerebro-pontine angle, lower leg, hand, abdominal wall, and larynx [2–4, 7, 8, 13–23, 25, 26, 28, 29]. By definition, STABC has no connection to the adjacent or underlying bone [16]. Twenty-seven cases (75%) were deep seated, either intramuscular or intermuscular, whereas others were superficial subcutaneous lesions [7]. None of our six STABC cases had a history of previous trauma. All were intramuscular tumors of the extremities (four cases), pelvis (one case), or abdominal wall (one case).

Fig. 4 Conventional radiograph of STABC. Antero-posterior radiograph of the left side of the pelvis (case 6). Mass projecting under the anterior iliac spine with discrete egg-shell mineralization along the periphery (arrows) (a). Antero-posterior radiograph of the upper leg (case 2) demonstrates a mass in the soft tissues surrounded by an ossified shell (b)



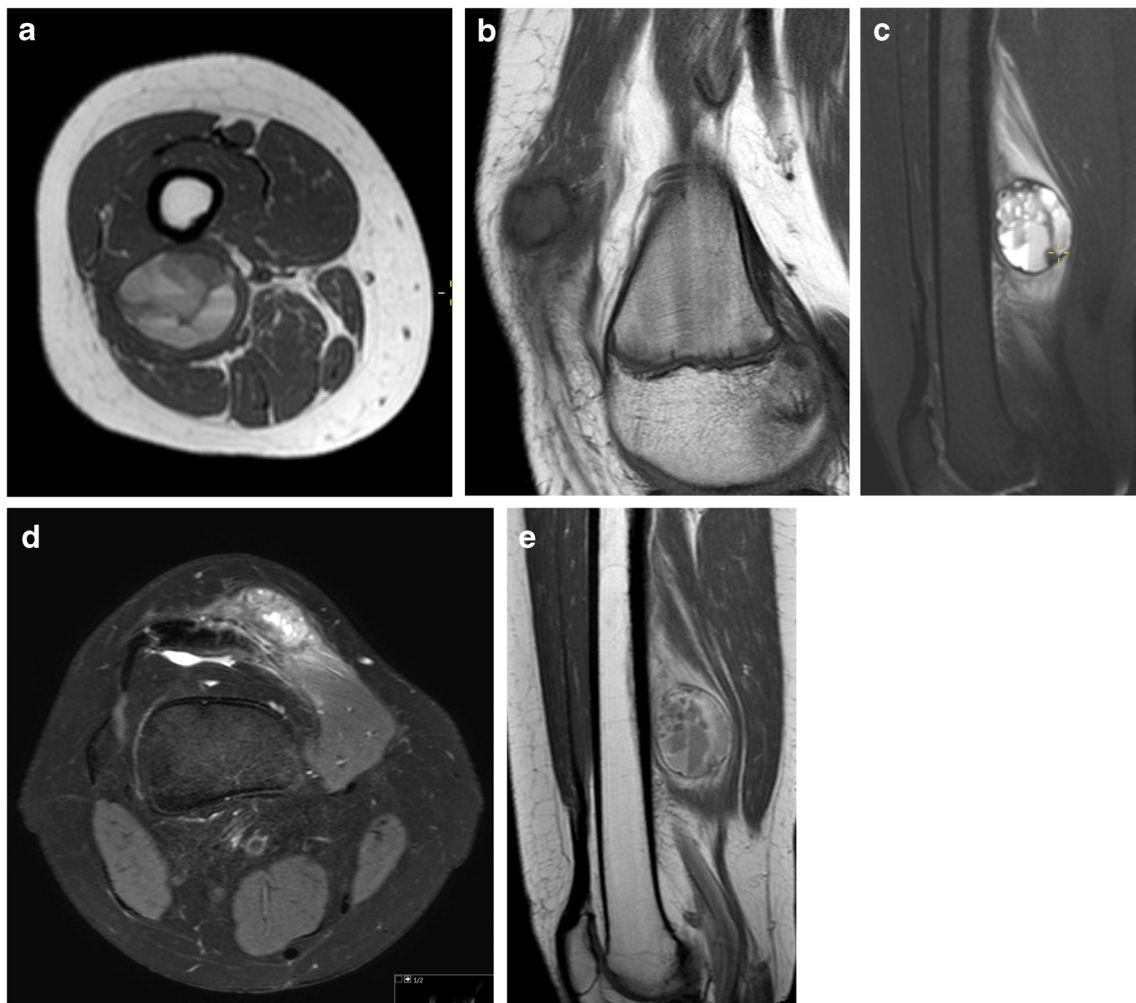


Fig. 5 MRI features of STABC. Axial T1-weighted image (case 1). Intramuscular mass in the short head of the biceps femoral muscle. Predominantly high signal intensity and multiple fluid-fluid levels (a). Sagittal T1-weighted MR image (case 3). Intramuscular lesion of intermediate signal intensity surrounded by a rim of low signal intensity caused by the peripheral calcification. Ill-defined stranding beyond this rim is caused by edema (b). Sagittal T2-weighted image with fat suppression (case 1). Intramuscular mass with predominantly high signal intensity and multiple fluid-fluid levels. Surrounding rim

of low signal intensity represents the egg-shell mineralization. Extensive ill-defined perilesional edema in the adjacent muscle tissue (c). Axial T2-weighted image with fat suppression (case 3). Intramuscular mass with predominantly high signal intensity surrounded by the low signal intensity rim from the peripheral calcification. Edema in the adjacent muscular tissue (d). Sagittal T1-weighted image after intravenous contrast administration (case 1). Septal enhancement within the lesion. Low signal intensity rim similar to the T2-weighted image. Enhancement of the edema (e)

Imaging features of STABC

Imaging features of our six STABC cases and the six cases reported in the radiological literature are summarized in Table 2. Peripheral mineralization was present in ten out of 12 cases (80%), either continuous or as an interrupted calcification [3, 8, 16–18, 25, 28]. In the majority of cases, the peripheral mineralization was eggshell-like. However, coarse peripheral ossification, similar to that encountered in myositis ossificans, may also occur [4, 13, 21, 29], as was seen in our case 4. Five STABC cases had a solid appearance, whereas seven STABC were multicystic with fluid-fluid levels found on MR in four cases (40%, see Table 2). On MR, the lesion

usually has an intermediate signal intensity on T1-weighted sequences and intermediate to high signal intensity on T2-weighted sequences, surrounded by a rim of low signal intensity on all sequences caused by the peripheral bone shell. In case of blood-filled spaces, the signal intensity was high on T1 with fluid-fluid levels, as was seen in our case 1. Septal enhancement was present in all three patients with a multicystic appearance on T2-weighted images that had post-contrast imaging. On MRI, nine lesions showed perilesional edema in adjacent soft tissues, which can lead to the impression of an aggressive or even malignant lesion. Some authors speculated that perilesional edema is only present in the active phase of STABC and disappears in a later, more quiescent stage. That

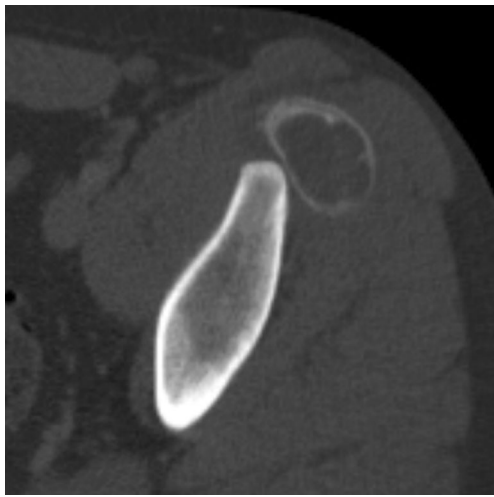


Fig. 6 CT image (case 6) with thin peripheral bone shell in the soft tissues anterior of the left iliac spine

may be deduced from the case described by Jacquot et al. [6] where MR was only performed late in the course of the disease and edema was absent. On CT, the shell of peripheral mineralization can easily be appreciated and usually is thin, but can be thicker and more coarse. On ultrasonography, the mass may demonstrate a cystic lesion with acoustic shadowing, depending on the presence of peripheral mineralization. Radionuclide imaging shows increased uptake of the radiotracer, as was present in three of our cases and the one reported by Jacquot et al. [6]. In two of our cases, the increased uptake was predominantly peripheral.

The radiological differential diagnosis of STABC mainly includes myositis ossificans. In STABC, however, the shell with peripheral mineralization is usually thin in contrast to the usually thicker and coarser peripheral mineralization in myositis ossificans. Importantly, on MRI scans, the presence

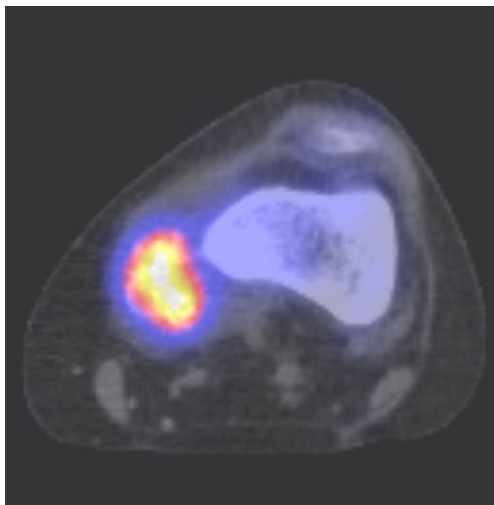


Fig. 7 SPECT fusion image (case 4) with diffuse increased uptake of the radiopharmakon within the lesion

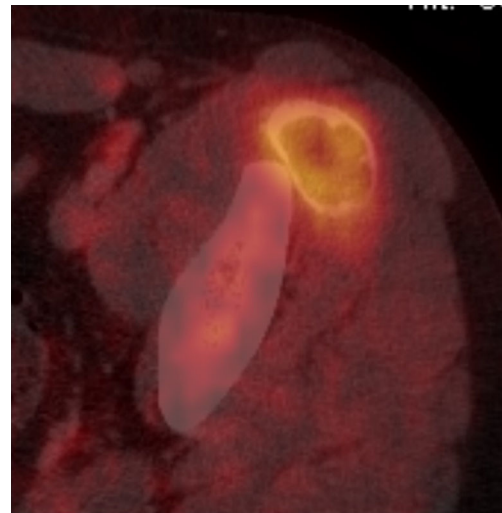


Fig. 8 The fused image of the PET-CT shows predominantly peripheral increased uptake of the radionuclide tracer (case 6)

of cavities, separated by septations, and fluid-fluid levels are very helpful to differentiate STABC from myositis ossificans [18, 21, 28]. Nevertheless, it can still be difficult to distinguish myositis ossificans from STABC on the basis of radiographic features only [18]. In some cases, such as in our cases 2–4, the cystic cavities, while apparent by gross and/or histological examination, were not visualized by MR imaging. By histology, the cysts of the three STABC cases had a diameter of 11 mm (case 2), 13 mm (case 3), and 1.7 mm (case 4). Given the spatial resolution of MRI, it may seem surprising that cysts larger than 1 cm were not visible with this imaging technique. We cannot exclude, however, that the cysts in these two STABC cases developed or increased in size in the period between imaging and surgery (4 and 7 months). Notably, our STABC case 4 appeared to be solid and a 1.7-mm ABC-like cyst was only discerned by microscopy of the previous needle biopsy, as shown in Fig. 1d. Thus, histology seems indispensable for a morphologic diagnosis of STABC as a distinct entity. Another tumor entering the radiological differential diagnosis because of the presence of a peripheral bone shell is ossifying fibromyxoid tumor (OFMT) [28]. However, OFMT is a solid tumor with a different histology and the majority of OFMT has *PHF1* gene rearrangements [30]. STABC should also be distinguished from liquefied hematoma and cavernous hemangioma, two lesions with cystic areas of high signal intensity on T1- and T2-weighted MR sequences. In addition, extraskeletal telangiectatic osteosarcoma may have fluid-fluid levels similar to those of soft tissue aneurysmal bone cyst [28]. Giant cell tumor of soft tissue should be included in the differential diagnosis, because this tumor may show secondary ABC formation. Notably, in one report, giant cell tumor of soft tissue with hemorrhage and large cystic degeneration was thought to represent STABC [27].

Histopathology and molecular pathology of STABC

The histological features of STABC are indistinguishable from those of ABC arising within bone [1, 18]. Histologically, STABC presents as a well-defined soft tissue mass consisting of cavernous spaces filled with blood and separated by fibrous septa, which lack smooth muscle or an endothelial lining, but contain osteoclast-type multinucleated giant cells, flattened spindle-shaped fibroblasts, and delicate reactive woven bone, often including so-called blue bone. STABC has a thin shell of bone [10, 16, 18, 20, 21]. The six STABC cases presented herein all had the distinct histologic features of STABC, as summarized in Table 1 and illustrated in Fig. 1a–f. Interestingly, after a diagnosis of STABC had been made on needle biopsy material available in case 4, the gross and microscopical features of the excised residual tumor were more reminiscent of myositis ossificans, and a *COL1A1-USP6* fusion gene was detected with NGS. Although ABC of bone and STABC have long been regarded as a reactive process, cytogenetic and molecular studies have provided evidence that (ST)ABC is a true neoplastic process [8, 16, 18, 28, 31, 32]. FISH can be used to demonstrate *USP6* rearrangements, whereas RT-PCR or anchored multiplex PCR-based targeted NGS may be used to detect the fusion partner. Importantly, using FISH, *USP6* rearrangement has also been found in myositis ossificans [33]. Some authors have questioned the specificity of *USP6* rearrangements in myositis ossificans and considered the possibility that these cases actually represent the early stage of soft tissue ABCs [31]. On the other hand, it was recently described that soft tissue lesions histologically diagnosed as myositis ossificans also have *USP6* rearrangements [33] and the fusion partner was *COL1A1* in 4/6 cases [34]. Thus, it appears that soft tissue lesions with *USP6* rearrangements, which include nodular fasciitis, myositis ossificans, and STABC may be part of a morphologic spectrum of the same biological entity. In fact, these lesions have overlapping morphologic features. Nodular fasciitis is a solid myofibroblastic neoplasm, with rare cases showing osteoclast-type giant cells and metaplastic bone formation. Myositis ossificans is a solid myofibroblastic tumor with extensive formation of lamellar trabecular bone via woven bone, whereas in STABC clear-cut cystic ABC areas are present, sometimes with areas of woven blue bone. Interestingly, our case 4 had overlapping features of STABC and myositis ossificans. With respect to *USP6* fusion genes, in nodular fasciitis the fusion partner is *MYH7*. In skeletal ABC, other fusion partners of *USP6* have been found, *CDH11* being the most frequent one (found in 30% of cases). Remarkably, in STABC only *COL1A1-USP6* fusions have been found so far (the three cases reported here and those described by Jacquot et al.). Moreover, Flucke et al. found co-existing *USP6* and *COL1A1* rearrangements in 4/6 tumors with features of myositis ossificans. More cases of myositis ossificans have to be studied to evaluate the significance of this observation.

In contrast to myositis ossificans, in which currently the therapy of first choice is non-surgical, the therapy of choice for STABC is wide local excision, given the growth potential of this lesion. Local recurrence is rare. In the literature, only two out of 36 tumors recurred after incomplete excision (5%) [2, 15]. Four patients were lost to follow-up [2, 3, 18, 19].

In conclusion, STABC is a rare soft tissue tumor, predominantly occurring in the upper leg and hip or upper arm and shoulder region and in a somewhat older age group than ABC of bone. Radiologically, STABC may present as a solid or cystic mass. Most often, an eggshell-thin mineralized layer surrounds STABC, but sometimes a coarser calcified layer similar to myositis ossificans is found. Perilesional edema is a prominent radiological feature on MR, which may erroneously suggest an aggressive or even malignant nature. Fluid-fluid levels were present in 40% of cases. Recently, it became apparent that STABC may belong to a spectrum of tumors with *USP6* gene rearrangement and *COL1A1-USP6* fusions, including myositis ossificans and nodular fasciitis. Clinically, the local recurrence rate of STABC is very low. It appears that only lesions that are excised incompletely may sometimes recur.

Authors' contributions Wangzhao Song studied the pathology specimens and drafted the manuscript with Stijn M. Bollen. Albert J. H. Suurmeijer conceived the study, participated in its design, and supervised this article. Anne-Marie Cleton-Jansen performed FISH and next-generation sequencing. Judith V.M.G. Bovée studied the pathology specimens and participated in the study design. Herman M. Kroon conceived the study, interpreted imaging features, designed, supervised, and finally approved this article. All authors read and approved the final manuscript.

Compliance with ethical standards

Conflict of interest No funds were received in support of this work. The authors declare that they have no conflicts of interest.

Sources of support W. Song receives funding from the China Scholarship Council (CSC) program (grant no: 201606940023).

Ethical approval All procedures performed in studies involving human participants were in accordance with the ethical standards of the institutional and/or national research committee and with the 1964 Helsinki Declaration and its later amendments or comparable ethical standards.

Informed consent Informed consent was obtained from all individual participants included in the study.

References

1. Jaffe HL, Lichtenstein L. Solitary unicameral bone cyst with emphasis on the roentgen picture, the pathologic picture and the pathogenesis. *Arch Surg*. 1942;46:1004–25.
2. Salm R, Sissons HA. Giant-cell tumours of soft tissues. *J Pathol*. 1972;107:27–39.
3. Ajillogba KA, Kaur H, Duncan R, McFarlane JH, Watt AJ. Extrasosseous aneurysmal bone cyst in a 12-year-old girl. *Pediatr Radiol*. 2005;35:1240–2.

4. Amir G, Mogle P, Sucher E. Case report 729. Myositis ossificans and aneurysmal bone cyst. *Skelet Radiol*. 1992;21:257–9.
5. Baker KS, Gould ES, Patel HB, Hwang SJ. Soft tissue aneurysmal bone cyst: a rare case in a middle aged patient. *J Radiol Case Rep*. 2015;9:26–35.
6. Jacquot C, Szymanska J, Nemana LJ, Steinbach LS, Horvai AE. Soft-tissue aneurysmal bone cyst with translocation t(17;17)(p13;q21) corresponding to COL1A1 and USP6 loci. *Skelet Radiol*. 2015;44:1695–9.
7. Samura H, Shiraishi M, Tokashiki H, Nosato E, Miyazato H, Muto Y. An extraosseous aneurysmal cyst in the pelvic cavity: report of a case. *Clin Imaging*. 2000;24:68–71.
8. Wang XL, Gielen JL, Salgado R, Delrue F, De Schepper AM. Soft tissue aneurysmal bone cyst. *Skelet Radiol*. 2004;33:477–80.
9. Van Eijk R, Stevens L, Morreau H, van Wezel T. Assessment of a fully automated high-throughput DNA extraction method for formalin-fixed, paraffin-embedded tissue for KRAS, and BRAF somatic mutation analysis. *Exp Mol Pathol*. 2013;94:121–5.
10. Meyers SP. MRI of bone and soft tissue tumors and tumorlike lesions—differential diagnosis and atlas. Stuttgart: Thieme Medical Publishers; 2008. p. 814.
11. Kransdorf MJ, Sweet DE. Aneurysmal bone cyst: concept, controversy, clinical presentation, and imaging. *AJR Am J Roentgenol*. 1995;164:573–80.
12. Martinez V, Sissons HA. Aneurysmal bone cyst. A review of 123 cases including primary lesions and those secondary to other bone pathology. *Cancer*. 1988;61:2291–304.
13. Hao Y, Wang L, Yan M, Jin F, Ge S, Dai K. Soft tissue aneurysmal bone cyst in a 10-year-old girl. *Oncol Lett*. 2012;3:545–8.
14. McCann KM, Clifford CE, Salton HL. Soft tissue aneurysmal bone cyst: a case report. *FAOJ*. 2011;4(6):No. 1.
15. Dal Cin P, Kozakewich HP, Goumnerova L, Mankin HJ, Rosenberg AE, Fletcher JA. Variant translocations involving 16q22 and 17p13 in solid variant and extraosseous forms of aneurysmal bone cyst. *Genes Chromosom Cancer*. 2000;28:233–4.
16. Karkuzhali P, Bhattacharyya M, Sumitha P. Multiple soft tissue aneurysmal cysts: an occurrence after resection of primary aneurysmal bone cyst of fibula. *Indian J Orthop*. 2007;41:246–9.
17. Lopez-Barea F, Rodriguez-Peralto JL, Burgos-Lizalde E, Alvarez-Linera J, Sanchez-Herrera S. Primary aneurysmal cyst of soft tissue. Report of a case with ultrastructural and MRI studies. *Virchows Arch*. 1996;428:125–9.
18. Nielsen GP, Fletcher CD, Smith MA, Rybak L, Rosenberg AE. Soft tissue aneurysmal bone cyst: a clinicopathologic study of five cases. *Am J Surg Pathol*. 2002;26:64–9.
19. Petrik PK, Findlay JM, Sherlock RA. Aneurysmal cyst, bone type, primary in an artery. *Am J Surg Pathol*. 1993;17:1062–6.
20. Riccioni L, Foschini MP. Extraosseous aneurysmal bone cyst. *Tumori*. 1996;82:485–7.
21. Rodriguez-Peralto JL, Lopez-Barea F, Sanchez-Herrera S, Atienza M. Primary aneurysmal cyst of soft tissues (extraosseous aneurysmal cyst). *Am J Surg Pathol*. 1994;18:632–6.
22. Shannon P, Bedard Y, Bell R, Kandel R. Aneurysmal cyst of soft tissue: report of a case with serial magnetic resonance imaging and biopsy. *Hum Pathol*. 1997;28:255–7.
23. D'Costa GF, Hastak MS, Patil YV. Primary aneurysmal cyst: bone type in the breast. *Indian J Surg*. 2007;69:248–50.
24. Della Libera D, Redlich G, Bittesini L, Falconieri G. Aneurysmal bone cyst of the larynx presenting with hypoglottic obstruction. *Arch Pathol Lab Med*. 2001;125:673–6.
25. Ellison DA, Sawyer JR, Parham DM, Nicholas R Jr. Soft-tissue aneurysmal bone cyst: report of a case with t(5;17)(q33;p13). *Pediatr Dev Pathol*. 2007;10:46–9.
26. Fellig Y, Oliveira AM, Margolin E, Gomori JM, Erickson-Johnson MR, Chou MM, et al. Extraosseous aneurysmal bone cyst of cerebello-pontine angle with USP6 rearrangement. *Acta Neuropathol*. 2009;118:579–81.
27. Lopez LV, Rodriguez MG, Siegal GP, Wei S. Extraskeletal aneurysmal bone cyst: report of a case and review of the literature. *Pathol Res Pract*. 2017;213:1445–9.
28. Pietschmann MF, Oliveira AM, Chou MM, Ihrler S, Niederhagen M, Baur-Melnyk A, et al. Aneurysmal bone cysts of soft tissue represent true neoplasms: a report of two cases. *J Bone Joint Surg Am*. 2011;93:e45.
29. Sahu A, Gujral SS, Gaur S. Extraosseous aneurysmal cyst in hand: a case report. *Cases J*. 2008;1:268.
30. Kao YC, Sung YS, Zhang L, Chen CL, Huang SC, Antonescu CR. Expanding the molecular signature of ossifying fibromyxoid tumors with two novel gene fusions: CREBBP-BCORL1 and KDM2A-WWTR1. *Genes Chromosom Cancer*. 2017;56:42–50.
31. Sukov WR, Franco MF, Erickson-Johnson M, Chou MM, Unni KK, Wenger DE, et al. Frequency of USP6 rearrangements in myositis ossificans, brown tumor, and cherubism: molecular cytogenetic evidence that a subset of “myositis ossificans-like lesions” are the early phases in the formation of soft-tissue aneurysmal bone cyst. *Skelet Radiol*. 2008;37:321–7.
32. Oliveira AM, Perez-Atayde AR, Dal Cin P, Gebhardt MC, Chen CJ, Neff JR, et al. Aneurysmal bone cyst variant translocations upregulate USP6 transcription by promoter swapping with the ZNF9, COL1A1, TRAP150, and OMD genes. *Oncogene*. 2005;24:3419–26.
33. Bekers EM, Eijkelenboom A, Grünberg K, Roverts RC, de Rooy JWW, van der Geest ICM, et al. Myositis ossificans—another condition with USP6 rearrangement, providing evidence of a relationship with nodular fasciitis and aneurysmal bone cyst. *Ann Diagn Pathol*. 2018;34:56–9.
34. Flucke U, Bekers EM, Creytens D, van Gorp JM. COL1A1 is a fusionpartner of USP6 in myositis ossificans—FISH analysis of six cases. *Ann Diagn Pathol*. 2018. <https://doi.org/10.1016/j.amdiagpath.2018.06.009>.